

## Enhancement of mobilities in a pinned multidomain crystal

Gwennou Coupier,<sup>1,\*</sup> Michel Saint Jean,<sup>1,†</sup> and Claudine Guthmann<sup>1</sup>

<sup>1</sup>*Laboratoire Matière et Systèmes Complexes, CNRS and Université Paris 7, 140 rue de Lourmel, 75015 Paris, France*

(Received 29 January 2007; published 5 June 2007)

Mobility properties inside and around degenerate domains of an elastic lattice partially pinned on a square array of traps are explored by means of a fully controllable model system of macroscopic particles. We focus on the different configurations obtained for filling ratios equal to 1 or 2 when the pinning strength is lowered. These theoretically expected but never observed configurations are degenerated, which implies the existence of a multidomain crystal. We show that the distinction between trapped and untrapped particles that is made in the case of strong pinning is not relevant for such a weaker pinning. Indeed, one ought to distinguish between particles inside or around the domains associated with positional degeneracies. The possible consequences on the depinning dynamics of the lattice are discussed.

DOI: [10.1103/PhysRevB.75.224103](https://doi.org/10.1103/PhysRevB.75.224103)

PACS number(s): 64.60.-i, 74.25.Qt

### I. INTRODUCTION

When submitted to an external force, an elastic lattice of interacting particles coupled to a regular array of pinning centers can move as soon as the applied force exceeds a threshold. The determination of this threshold and of the behavior of the elastic lattice near it is important and current questions. This threshold essentially depends on two parameters: the local deviations of the particles with respect to their positions in the unpinned lattice and the local energetic landscape around the pinned equilibrium configuration. Thus, knowing how this deformation will take place and exploring how the particles locally move around their pinned positions in equilibrium configurations is a first step toward the understanding of the lattice depinning process.

In this paper, we show how the existence of multidomain configurations would act on the dynamics of an elastic lattice pinned by a periodic potential of medium amplitude. In order to explore this question, we have developed an experimental system allowing the direct observation of the interacting particles and a well controlled pinning process. It will also be presented.

Many elastic systems submitted to a pinning array have been explored for some years. The most studied of them are the flux lattices in superconductors since a good pinning of the vortices increases the critical current in the material. Recently, the focus on such questions has grown since progress in lithography techniques on superconducting thin materials has offered the opportunity to design arrays of holes or magnetic dots, which act as strong pinning centers where one vortex or even more can be trapped;<sup>1-6</sup> this procedure is much more efficient and potentially controllable than the weak pinning resulting from intrinsic defects in the material.<sup>7</sup> In such a situation, a key parameter is the ratio  $f$  between the vortex density, which is controlled by the magnetic-field intensity, and the pinning center density. Indeed, measurements of macroscopic characteristics such as the voltage-current response or of the vortex lattice melting temperature have shown unambiguously that they strongly depend on  $f$  for a square or triangular pinning array and that the pinning is more efficient for rational  $p/q$  values of  $f$ , where  $p$  and  $q$  are small.<sup>8</sup>

The dependence of the depinning threshold on the microscopic vortex organization and their dynamics has been proved through semianalytic or numerical works that were first devoted to the static problem of the pinned lattice configuration.<sup>9-14</sup> Taking the lowest-energy equilibrium configuration as a starting point, the different phases of a driven moving lattice have been simulated;<sup>11,12,15,16</sup> the resulting quasi-one-dimensional movement has also been specifically studied.<sup>17</sup> Let us emphasize at this point that, whereas in most cases, the equilibrium configurations are degenerate; the possible existence of multidomain lattices is seldom taken into account in these numerical studies.<sup>18</sup> We shall see that it could be a problem since particles' behaviors strongly differ depending on whether they are inside the domains or in the walls between them.

From the experimental point of view, investigating the microscopic configurations of a vortex lattice is still a challenging issue. The best imaging of equilibrium configurations has been obtained with scanning Hall probe,<sup>2-5</sup> scanning tunneling,<sup>6</sup> or Lorentz<sup>1</sup> microscopy. In these works, configurations of mainly some hundreds of vortices are imaged for rational filling ratios  $f$  close to 1 ( $1/4 \leq f \leq 4$ ). However, even though great efforts have been made in this way, a direct imaging of (pinned) vortex lattices suffers from two major drawbacks. First, it is presently impossible to track the vortices and follow their dynamics; furthermore, the nature of the artificial pinning centers used in the works cited above does not offer the required experimental facility to control the amplitude and the shape of the pinning potential.

Therefore, a complementary approach based on similar systems has appeared to be necessary. Beyond their intrinsic interest, colloidal crystals can be seen as an attractive alternative solution. The first attempts in this way have recently involved colloidal crystals pinned by arrays of optical traps. Nevertheless, the observed configurations, which are also numerically predicted,<sup>19,20</sup> are to date either quite different than the one observed in superconductors<sup>21</sup> or restricted to system of very small spatial extent.<sup>22</sup> Moreover, the role of the hydrodynamic couplings and of the nature of the pinning strength is, in these systems, still unclear.

In order to bypass these difficulties, we propose here an alternative experimental system consisting of a few thousand

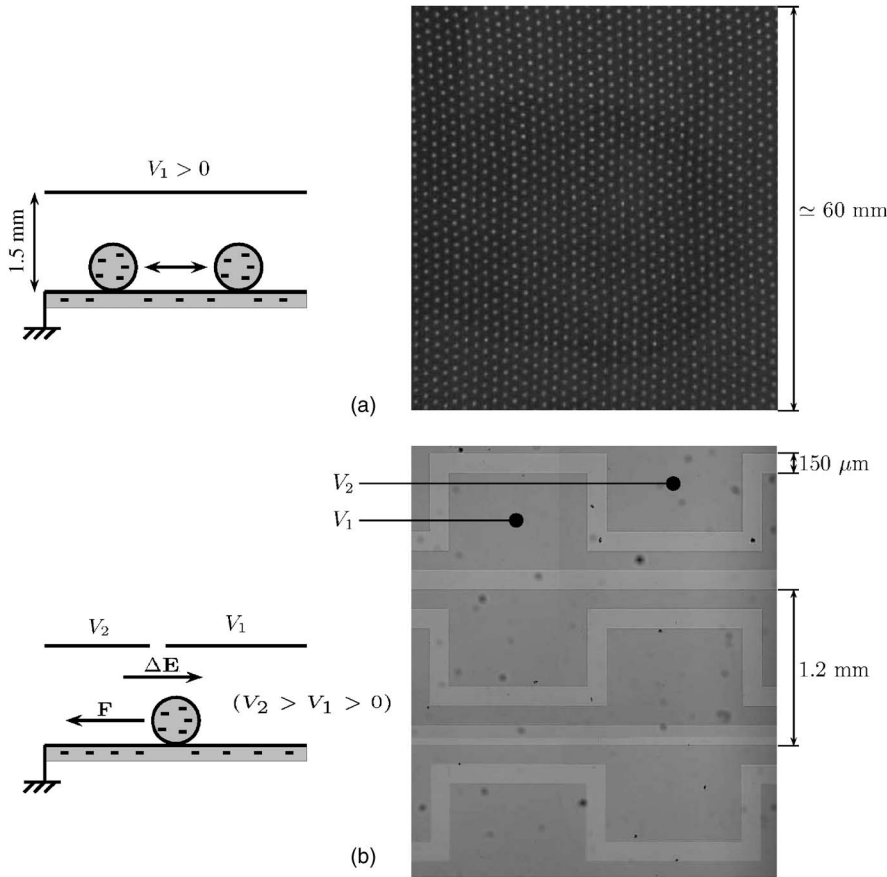


FIG. 1. Summary of the two electrostatic forces at stack. (a) Scheme accounting for the origin of the repulsive interaction between two balls and picture of the resulting triangular lattice. (b) Scheme accounting for the apparition of the pinning force under two areas linked to two different potentials and picture of a few adjacent patterns in the indium tin oxide electrode that is used to study the  $f=1$  case.

millimetric charged particles which can be submitted to a controlled electrostatic pinning potential and a tunable effective temperature resulting from a mechanical shaking. After a brief description of the pinning setup and the experiments which validate its efficiency (Sec. II), we present in Sec. III the multidomain equilibrium configurations and their evolution when the amplitude of the pinning strength decreases in the case of a square array of traps. We mainly focus on the  $f=1$  and  $f=2$  cases. Finally, the thermally activated motion of the particles in these multidomain systems is described and discussed in Sec. IV.

## II. EXPERIMENTAL SETUP

The system we propose, a so-called “pinned macroscopic Wigner crystal,” is made of a monolayer of confined charged millimetric balls. These conducting balls are located on the grounded bottom electrode of a horizontal plane condenser. When a tunable voltage  $V_1 > 0$  ( $V_1 \approx 1$  kV) is applied between the top and the bottom electrodes, the balls get negatively charged and repel each other [Fig. 1(a)]. In Ref. 23, we have shown that the interball interaction potential  $E(r)$  is equal to  $E_0 K_0(r/\lambda)$ , where  $K_0$  is the modified Bessel function of the second kind, and  $E_0$  is proportional to  $V_1^2$ . This interaction between the balls has the same space dependence as the interaction between vortices in superconductors, which suggests that the observed behaviors could be directly mapped onto vortex systems without the experimental constraints associated with the real ones. To introduce thermal

noise, the whole cell is fixed on loudspeakers supplied by a white-noise voltage. We have thoroughly checked that the resulting shaking of the balls, due to friction with the bottom electrode, fulfills the properties one can expect for a thermal shaking. Firstly, even though all the balls lie on the same solid substrate, their movement is spatially noncorrelated, which might be due to inhomogeneities on the wafer at a microscopic level. Secondly, the individual trajectory of a single ball which is free or trapped in a parabolic well can be described through Langevin formalism.<sup>24</sup> Stationary states are reached in a few tenth of second. They are characterized by an effective temperature directly controlled by the shaking amplitude: the energy distribution is given by Boltzmann statistics. This was proved on confined small islands of balls that can be seen as two-level systems when considering their two first equilibrium configurations, characterized by concentric shells of varying number of balls.<sup>25</sup> This effective temperature was calibrated and is measured *in situ*.

When submitted to a low effective temperature, the ensemble of balls can organize and form a defect-free triangular lattice of a few thousand particles.<sup>26</sup> By insulating a periodic set of small patterns in the top electrode, we can link it to a different tunable voltage  $V_2 > V_1$ , and create an array of pinning sites, as the local potential difference results in an attractive force on a ball [Fig. 1(b)]. Since the net charge on the ball around the trap is roughly proportional to the mean potential  $V$  between  $V_1$  and  $V_2$ , the amplitude of the pinning potential can be considered as proportional to  $V\Delta V$ , where  $\Delta V = V_2 - V_1$  comes from the gradient of the electrostatic potential between the inside and the outside of the trap. There-

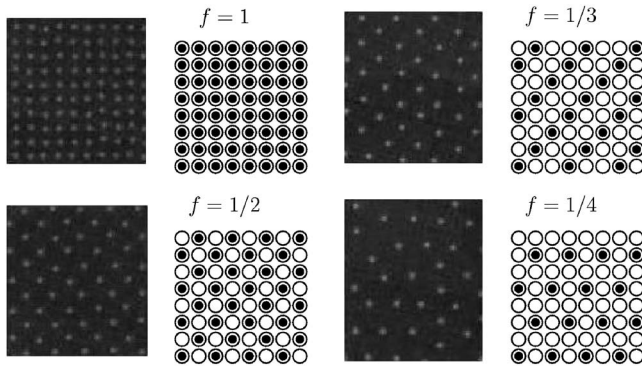


FIG. 2. Overview of the equilibrium configurations on a square array with filling ratios equal to 1, 1/2, 1/3, and 1/4. The corresponding theoretical schemes for a monodomain configuration are also shown. The traps are represented by empty circles, while the black disks represent the particles.

fore, the relevant parameter to discuss the relative strength of the pinning compared with the elastic stiffness will be  $\eta_V = V\Delta V/V^2 = \Delta V/V$ , which is fully controlled.

In our experiments, the lattice spacing  $a_0$  in the unpinned lattice (made of nearly 2000 balls) is 1.82 mm, to be compared with the screening length  $\lambda = 0.48$  mm. The periodicity of the square pinning array is then chosen so that the filling ratio  $f$  is equal to 1 or 2. The width of the patterns is such that the range of the pinning potential associated with one site is of the same order as the interball distance.

In order to test first the efficiency of this pinning device, we have observed the equilibrium configurations obtained when starting from  $f=1$  and taking off some balls so that  $f \leq 1$ , with high values for the relative pinning strength ( $\eta_V \geq 0.25$ ). These configurations have been compared to those reported in the literature.

Our experimental equilibrium configurations are shown for some fractional filling ratios in Fig. 2 for a square pinning array and in Fig. 3 for a triangular array. In the first case, they are similar to those observed in superconductors<sup>1,4,5</sup> and numerically predicted.<sup>11,14</sup> In the second case, they are also similar to those numerically predicted.<sup>11</sup> These results confirm the ability of our system to be generic of elastic systems and to describe well the behavior of flux lattices in superconductors.

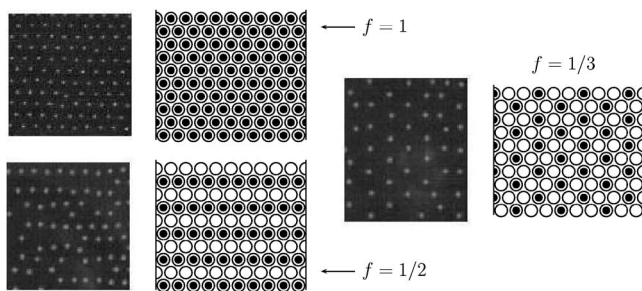


FIG. 3. Overview of the equilibrium configurations and corresponding schemes for a triangular array with filling ratios equal to 1, 1/2, and 1/3.

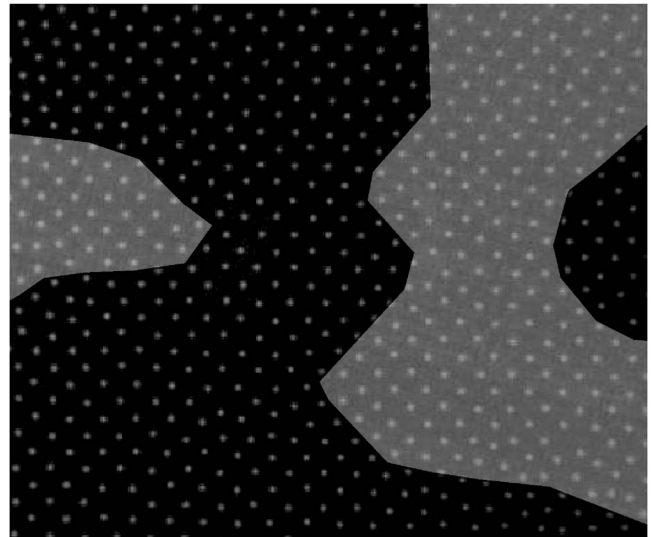


FIG. 4. Snapshot of the crystal in a quasiequilibrium state with  $f=1/2$  and a square pinning array. The theoretical configuration is twofold degenerate, which leads to the existence of two kinds of domains (black and gray background colors).

### III. MULTIDOMAIN EQUILIBRIUM CONFIGURATIONS

The existence of multidomain equilibrium configurations depends on different parameters.

For  $f < 1$ , the equilibrium configurations are structurally degenerate since the organized pinned lattice can be pinned on various subarrays of traps whatever the shape and the intensity of the pinning potential. Therefore, it is experimentally difficult to obtain large coherent domains, and multidomain systems are often observed as, for instance, in our system (Fig. 4), or in superconductors, where a multidomain experimental configuration of a  $f=1/2$  crystal of more than  $10^4$  vortices has clearly been imaged.<sup>4</sup> On the contrary, according to what is stated in Ref. 11, it seems to be difficult to find these multidomain configurations through numerical simulations.

Beyond these easily predictable cases, theoretical studies suggest that for  $f \geq 1$ , lowering the amplitude of the pinning strength or widening the traps can lead to partially pinned (PP) configurations, where only a fraction of the vortices are located in the middle of the pinning sites,<sup>14</sup> allowing multidomain configurations. Such configurations have never been observed in superconductors, perhaps because the pinning intensity is too high; however, our experiments in which the pinning strength can be tuned confirm this assumption.

For  $f=1$ , a sharp transition between the totally pinned (TP) and the partially pinned configuration is observed when lowering  $\eta_V$  ( $\eta < 0.15$ ). The latter configuration consists in an alternation of rows of trapped or untrapped balls, so that the triangular symmetry of the unpinned lattice is almost restored, the position of the untrapped particle between two free traps slightly depending on the relative pinning strength (Fig. 5). Let us now emphasize that this partially pinned configuration is degenerate since there are two possibilities for the orientation of the unpinned rows (Fig. 6).

Note that we do not discuss here the existence of a “floating crystal,” a triangular lattice slightly distorted by the

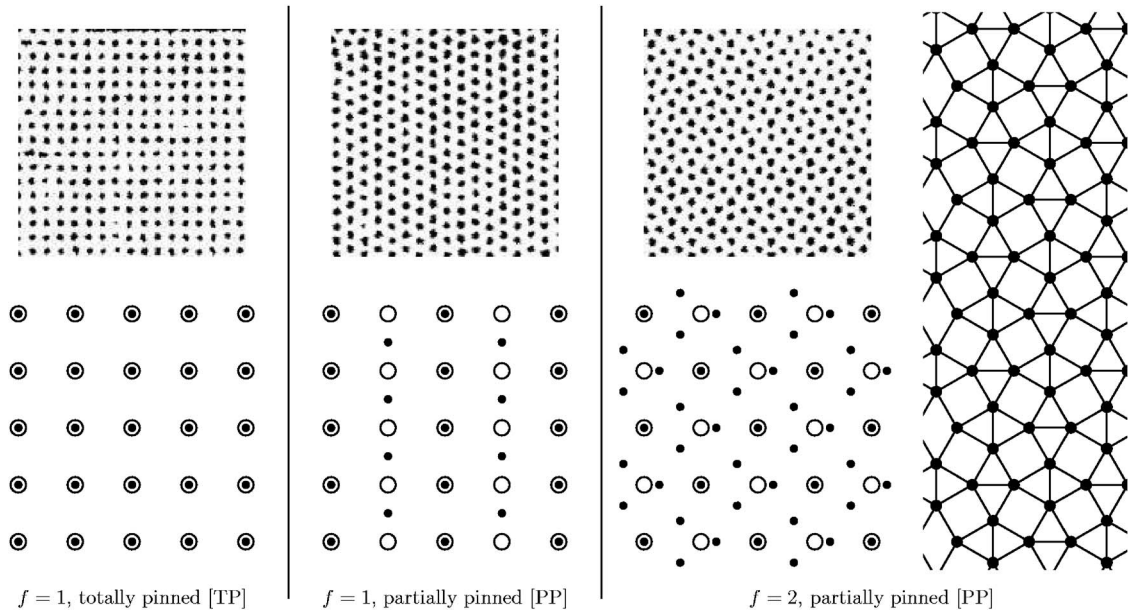


FIG. 5. Thermally activated trajectories around equilibrium configurations and corresponding schemes. For  $f=1$ , the transition between both configurations is obtained by tuning  $\eta_V$ . The Delaunay triangulation of the partially pinned configuration for  $f=2$  is also shown.

traps: in the literature, its orientation is controversial, as it can be aligned with the axes of the underlying pinning array,<sup>15</sup> or slightly rotated.<sup>14</sup> Experimentally, this orientation should depend strongly on the boundary conditions, unlike the pinned configurations. Anyhow, as for  $f=1$ ,<sup>14</sup> one should expect this configuration to be favored when the traps widen and can include many particles: then, a triangularlike structure will be obviously preferred.

In the  $f=2$  case, a “totally pinned” configuration, where all the traps are occupied and the remaining particles are located in the center regions between the traps, is usually observed in superconductors,<sup>1,2</sup> and also numerically predicted.<sup>9</sup> We have also obtained this configuration with a strong pinning ( $\eta \geq 4$ ). For traps with larger extent, totally pinned configurations switch to a regular array of dimers centered on the traps, as it was shown by numerical simulations for vortices with logarithmic interaction.<sup>10</sup> This configuration could be the one observed by Field *et al.*, where two flux quanta are trapped in each pinning center.<sup>4</sup> Similar configurations seem to be also observed in colloidal systems. Indeed, the latter affirmation is an extrapolation of the observations made in Ref. 21, where the  $f=3$  case is studied and an array of trimers is observed. This extrapolation is confirmed by numerical simulations made by Reichhardt and Olson<sup>19</sup> In these cases, the degeneracy is linked to the rotation of the dimers, while the TP configuration is not degenerate. These results indicate that the existence of multidomain systems depends on the intensity and the shape of the pinning potential.

Since in our experiment we can tune the pinning intensity (the trap shape being fixed), we have explored the evolution of the TP configuration as this intensity decreases. For not too high values of  $\eta_V$ , we have observed an unexpected and interesting PP configuration shown in Fig. 5. Only half the traps are occupied while the others are the centers of trimers, effectively trapping three particles instead of one. An elegant

fourfold configuration results in which each particle has got exactly five equidistant neighbors. These patterns result from a compromise between the symmetry imposed by the pinning array and the symmetry of the unpinned lattice, which is sixfold. Since there are two possibilities for the choice of the subarray of occupied traps and, for each selected subarray, four possibilities for the orientation of the trimers, the system is highly degenerated and, as a consequence, a multidomain configuration will appear in the pinned lattice.

The multidomain partially pinned configurations are observed in our whole system as shown in Fig. 6 for  $f=1$  and Fig. 7 for  $f=2$ , where three domains are present. In the latter, the difference between domains I and II lies in the choice of the occupied subarray. Between domains II and III, the trimers do not have the same orientation. In both cases, the walls are marked by features looking like “eyes” constituted by a well trapped particle surrounded by very mobile ones. We shall return to this last point in the following.



FIG. 6. Thermally activated trajectories in a multidomain partially pinned configuration for  $f=1$ .

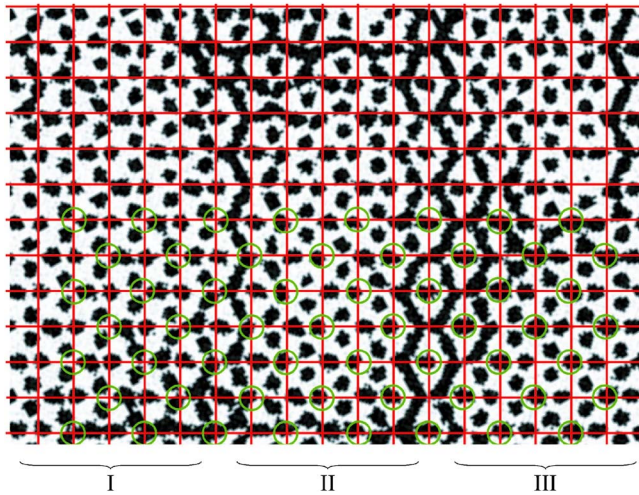


FIG. 7. (Color online) Thermally activated trajectories in a multidomain partially pinned configuration for  $f=2$ . The traps are located at the intersections of the lines. The circles mark one of the two subarrays that can be occupied by particles.

In these configurations, the domains' sizes increase for high  $V$ , thus for high intensities of the forces at stack. Notice furthermore that these configurations are highly symmetric, the walls between the domains being mainly orientated along the principal axes of the pinning lattice. These equilibrium multidomain configurations are very stable and can be considered as quasistatic because of the presence of pinned particles. The evolution in shape and size of each domain is much slower than in the case of a disoriented cluster in an unpinned lattice that was discussed in Ref. 26.

In order to determine the conditions required to observe such configurations, we have calculated the phase diagrams of the pinned macroscopic Wigner lattices, the two relevant parameter being the relative pinning intensity  $E_p/E_0$  and the width  $\sigma$  of each electrostatic trap.

Since the analytical determination of these attracting potentials is a tricky problem, we have calculated the phase diagram for different profile and compared them to the experimental results.

This procedure is relevant to find the depth  $E_p$  and width  $\sigma$  of the traps since the obtained phase diagrams strongly differ according to the choice in the profile used for its calculation, as it was shown in Ref. 14 for  $f=1$ .

Various shapes have been proposed in the literature: in the numerical simulations of flux lattices, this potential is either a truncated parabola or a Gaussian,<sup>9-11,14</sup> whereas the optical traps in colloidal systems seem to be well described by sine functions.<sup>19</sup> Our calculations show that a good agreement is obtained for traps with Gaussian profiles  $E_g(r) = -E_p \exp \times [-r^2/(2\sigma^2)]$ .

In particular, using this trap profile, we have calculated the phase diagram for  $f=2$  for which we consider three possible configurations: the totally pinned configuration, the partially pinned one, and the dipole configuration found in Ref. 10. The resulting phase diagram for a Gaussian profile is shown in Fig. 8.

It can be seen from the diagram that the partially pinned configuration is favored relative to the totally pinned one for

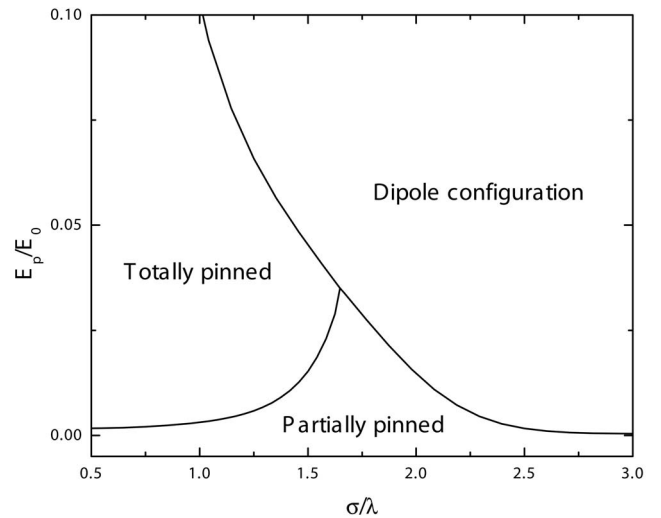


FIG. 8. Phase diagram for the three pinned configurations that are found here and in the literature for  $f=2$  and a square pinning array. The values for  $a_0$  and  $\lambda$  are the experimental ones. The profile of the wells is Gaussian, with a depth  $E_p$  and a width  $\sigma$ .

sufficiently wide or shallow traps. Perhaps, the dipole configuration could not be observed in our system because the traps are not wide enough or because  $\eta_V$  has an upper bound by construction.

Let us nevertheless indicate that such a phase diagram has to be considered more as a guide for the experiment than a tool for precise predictions: indeed, these phase diagrams are sensitive to the details of the unknown profile of the traps and one cannot assert that the real traps in our experiments or in flux lattices can be described by the simple functions that are usually tried.

#### IV. PARTICLE DYNAMICS BETWEEN AND ALONG THE DOMAIN WALLS

The presence of quasistatic domains leads to the existence of two kinds of particles, viz., those inside the domains and those near the walls. As discussed by Grigorenko *et al.*,<sup>5</sup> lacking or excess particles are required for the adjustment of the domains and the construction of the walls. Thus, these two kinds of particles are associated with different local densities. Our experiments show that even if these density variations are tiny, they induce important differences in the dynamics of the balls, even in the absence of an external force. More precisely, the movements in or alongside the domains strongly differ from the view of the associated mobility and the direction of the movement.

In the  $f=2$  case (Fig. 7), if one first looks inside the domains, the trapped or untrapped balls (viz., those belonging to a trimer) are stable and their dynamics essentially result from the thermal activation. As it can be seen on the trajectory spots, the amplitude of the movements of the trapped or of the trimer particles is equal. We can conclude from this result that the particle status toward the traps is not relevant to discuss its dynamical properties. Underline that this behavior can be associated with the conditions under which the

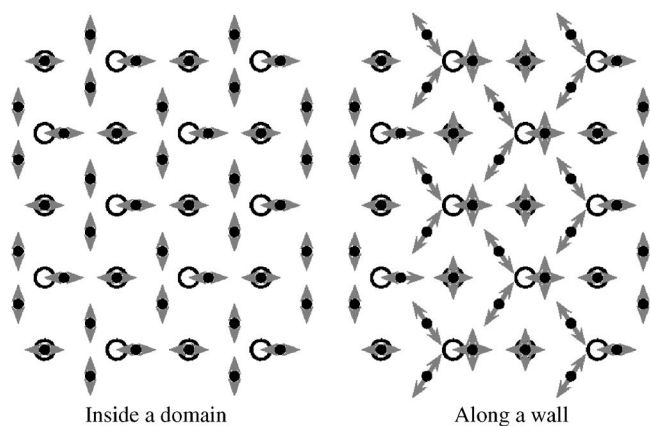


FIG. 9. Schemes of the main movement of the particles inside a domain or along a domain wall at low temperature. Note that the lacking or excess particles of the wall are not represented.

partially pinned configuration is energetically favorable, notably the necessity to have wide traps. In already studied totally pinned configurations,<sup>15,22</sup> interstitial particles are much more mobile than trapped ones.

The dynamics along the walls is pretty different. Indeed, the eyes in the walls are constituted by a well trapped particle, whose wandering amplitude is similar to the one inside a domain, surrounded by much more mobile untrapped particles. This high mobility can be associated with the local metastability linked with a small density variation. This makes the fact that the trapped particles remain in their place and are not chased by their neighbors all the more surprising.

Furthermore, the favored directions are also pretty different according to the class of the particles. These directions are schematized in Fig. 9. Inside a domain, all the movements have a privileged direction following the symmetry of the underlying pinning array. Notice that for the untrapped balls, this movement is surprising since it is not orientated toward the traps. This appears clearly when the temperature increases, the symmetry of the underlying pinning array being then directly recovered through the trajectories mapping (Fig. 10). Note that this is completely different than the “two-stage melting” that is found in the dipole configuration.<sup>10</sup> On the other hand, the untrapped particles near a metastable area are clearly following trajectories linking two adjacent empty pinning centers. We think that this phenomenon should be directly linked with the existence of

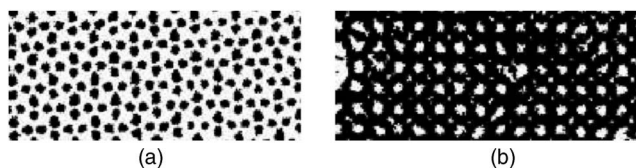


FIG. 10. Trajectories inside a homogeneous domain of the partially pinned configuration for  $f=2$ . In (b), the temperature is twice the temperature in (a).

trimers which are in a very uncomfortable position and are highly perturbed by a density variation. By contrast, for  $f=1$ , the movements along the walls are also enhanced relative to the movements inside the domains but are still respecting the same fourfold underlying symmetry as inside the domains (Fig. 6).

As a conclusion, this study performed with a macroscopic Wigner crystal has shown without ambiguity that the existence of domains must be taken into account to discuss the particle dynamics in a pinned elastic lattice. Those multidomain configurations appear as soon as the pinning amplitude diminishes and implies degenerate equilibrium configurations. The tracking of the particles has shown that the discrimination that should be made between trapped and interstitial particles in the totally pinned case is not relevant in a weaker pinning case for which one should discuss the dynamics by discriminating between particles in stable or metastable situations, respectively, inside or at the boundaries of the domains. This suggests that the existence of domains must be taken into account in further experimental or numerical studies of the moving phases of a partially pinned lattice submitted to a depinning force. Consequences could be first an easier depinning along the walls, which would then induce anisotropy since the orientations of the walls are given by the principal axes of the pinning array. In return, depinning of the lattice could remove the degeneracies, which would then imply isotropy. In Ref. 11, the nature of the flow is discussed according to the values of the filling ratio  $f$ . It is shown that if  $f$  is rational, this flow has elastic properties, whereas plasticity is invoked when  $f$  is irrational. Even though the “macroscopic filling ratio” is rational here, the local ratio near the boundaries is irrational and thus, the nature of the depinning dynamics could become very complex with a coexistence of elastic and plastic flows in the same lattice.

\*Present address: Laboratoire de Spectrométrie Physique, CNRS and Université Joseph Fourier, Grenoble, B.P. 87, 38402 Saint-Martin d’Hères, France.

†Electronic address: michel.saintjean@paris7.jussieu.fr

<sup>1</sup>K. Harada, O. Kamimura, H. Kasai, T. Matsuda, A. Tonomura, and V. V. Moshchalkov, *Science* **271**, 1167 (1996).

<sup>2</sup>A. N. Grigorenko, G. D. Howells, S. J. Bending, J. Bekaert, M. J. Van Bael, L. Van Look, V. V. Moshchalkov, Y. Bruynseraede, G. Borghs, I. I. Kaya, and R. A. Stradling, *Phys. Rev. B* **63**, 052504

(2001).

<sup>3</sup>D. M. Silevitch, D. H. Reich, C. L. Chien, S. B. Field, and H. Shtrikman, *J. Appl. Phys.* **89**, 7478 (2001).

<sup>4</sup>S. B. Field, S. S. James, J. Barentine, V. Metlushko, G. Crabtree, H. Shtrikman, B. Ilic, and S. R. J. Brueck, *Phys. Rev. Lett.* **88**, 067003 (2002).

<sup>5</sup>A. N. Grigorenko, S. J. Bending, M. J. vanBael, M. Lange, V. V. Moshchalkov, H. Fangohr, and P. A. J. deGroot, *Phys. Rev. Lett.* **90**, 237001 (2003).

- <sup>6</sup>G. Karapetrov, J. Fedor, M. Iavarone, D. Rosenmann, and W. K. Kwok, *Phys. Rev. Lett.* **95**, 167002 (2005).
- <sup>7</sup>Reviews on the specific problems that are encountered in elastic lattices pinned by random potential can be found in T. Giamarchi and P. Le Doussal, in *Spin Glasses and Random Fields*, edited by A. P. Young (World Scientific, Singapore, 1997); T. Giamarchi and S. Bhattacharya, in *High Magnetic Films: Applications in Condensed Matter Physics and Spectroscopy*, edited by C. Berthier, L. Levy, and G. Martinez (Springer, New York, 2002); Some examples of numerical simulations can be found in C. J. Olson, C. Reichhardt, and F. Nori, *Phys. Rev. Lett.* **81**, 3757 (1998); A. B. Kolton, D. Domínguez, and N. Grønbech-Jensen, *ibid.* **83**, 3061 (1999); H. Fangohr, S. J. Cox, and P. A. J. de Groot, *Phys. Rev. B* **64**, 064505 (2001); M. Chandran, R. T. Scalettar, and G. T. Zimányi, *ibid.* **67**, 052507 (2003); E. Olive and J. C. Soret, *Phys. Rev. Lett.* **96**, 027002 (2006).
- <sup>8</sup>An exhaustive list of references for works dealing with the macroscopic signatures of these matching effects can be found in U. Welp, X. L. Xiao, V. Novosad, and V. K. Vlasko-Vlasov, *Phys. Rev. B* **71**, 014505 (2005).
- <sup>9</sup>C. Reichhardt, C. J. Olson, and F. Nori, *Phys. Rev. B* **57**, 7937 (1998).
- <sup>10</sup>C. Reichhardt and N. Grønbech-Jensen, *Phys. Rev. Lett.* **85**, 2372 (2000).
- <sup>11</sup>C. Reichhardt and N. Grønbech-Jensen, *Phys. Rev. B* **63**, 054510 (2001).
- <sup>12</sup>C. Reichhardt, G. T. Zimányi, and N. Grønbech-Jensen, *Phys. Rev. B* **64**, 014501 (2001).
- <sup>13</sup>M. F. Laguna, C. A. Balseiro, D. Dominguez, and F. Nori, *Phys. Rev. B* **64**, 104505 (2001).
- <sup>14</sup>W. V. Pogosov, A. L. Rakhmanov, and V. V. Moshchalkov, *Phys. Rev. B* **67**, 014532 (2003).
- <sup>15</sup>C. Reichhardt, C. J. Olson, R. T. Scalettar, and G. T. Zimányi, *Phys. Rev. B* **64**, 144509 (2001).
- <sup>16</sup>C. Reichhardt, C. J. Olson, and F. Nori, *Phys. Rev. B* **58**, 6534 (1998); J. E. Villegas, S. Savel'ev, F. Nori, E. M. Gonzalez, J. V. Anguita, R. García, and J. R. Vicent, *Science* **302**, 1188 (2003); B. Y. Zhu, F. Marchesoni, and F. Nori, *Phys. Rev. Lett.* **92**, 180602 (2004); C. J. Olson Reichhardt and C. Reichhardt, *Physica C* **432**, 125 (2005); C. J. Olson Reichhardt, A. Libal, and C. Reichhardt, *Phys. Rev. B* **73**, 184519 (2006); D. Cole, S. Bending, S. Savel'ev, A. Grigorenko, T. Tamegai, and F. Nori, *Nature (London)* **5**, 305 (2006); F. Nori and S. Savel'ev, *Physica C* **437-438**, 226 (2006); Q. H. Chen, G. Teniers, B. B. Jin, and V. V. Moshchalkov, *Phys. Rev. B* **73**, 014506 (2006).
- <sup>17</sup>S. Anders, A. W. Smith, H. M. Jaeger, R. Besseling, P. H. Kes, and E. van der Drift, *Physica C* **332**, 35 (2000); R. Besseling, R. Niggebrugge, and P. H. Kes, *Phys. Rev. Lett.* **82**, 3144 (1999); R. Besseling, P. H. Kes, T. Dröse, and V. M. Vinokur, *New J. Phys.* **7**, 71 (2005); N. Kokubo, R. Besseling, V. M. Vinokur, and P. H. Kes, *Phys. Rev. Lett.* **88**, 247004 (2002); N. Kokubo, R. Besseling, and P. H. Kes, *Phys. Rev. B* **69**, 064504 (2004); S. J. Bending, G. D. Howells, A. N. Grigorenko, M. J. van Bael, J. Bekaert, K. Temst, L. V. Look, V. V. Moshchalkov, Y. Bruynseraede, G. Borghs *et al.*, *Physica C* **332**, 20 (2000).
- <sup>18</sup>This might be due to the limited number of particles that simulations are able to deal with up to date.
- <sup>19</sup>C. Reichhardt and C. J. Olson, *Phys. Rev. Lett.* **88**, 248301 (2002).
- <sup>20</sup>M. Mikulis, C. J. Olson Reichhardt, C. Reichhardt, R. T. Scalettar, and G. T. Zimányi, *J. Phys.: Condens. Matter* **16**, 7909 (2004); C. Reichhardt and C. J. Olson Reichhardt, *Proc. SPIE* **5514**, 352 (2004); *Europhys. Lett.* **68**, 303 (2004); *Phys. Rev. E* **71**, 062403 (2005).
- <sup>21</sup>M. Brunner and C. Bechinger, *Phys. Rev. Lett.* **88**, 248302 (2002).
- <sup>22</sup>K. Mangold, P. Leiderer, and C. Bechinger, *Phys. Rev. Lett.* **90**, 158302 (2003).
- <sup>23</sup>P. Galatola, G. Coupier, M. Saint Jean, J.-B. Fournier, and C. Guthmann, *Eur. Phys. J. B* **50**, 549 (2006).
- <sup>24</sup>G. Coupier, M. Saint Jean, and C. Guthmann, *Phys. Rev. E* **73**, 031112 (2006).
- <sup>25</sup>G. Coupier, C. Guthmann, Y. Noat, and M. Saint Jean, *Phys. Rev. E* **71**, 046105 (2005).
- <sup>26</sup>M. Saint Jean, C. Guthmann, and G. Coupier, *Eur. Phys. J. B* **39**, 61 (2004).